Proceedings RootS25
3rd International Workshop on Soil-Vegetation-Atmosphere Interaction
Boldrin D, Cecconi M, Cotecchia F, Leung A, Pedone G, Perrini P, Romero E, Tagarelli V, Zdravković L (eds)
ISSN: 3107-300X

doi: doi.org/10.53243/RootS2025-13

Root and fibre reinforcement impacts on pore dynamics and water storage capacity

F. Anselmucci[1], H. Cheng[1], M. Alam[2], A. Das[2], V. Magnanimo[1]

[1]*Chair of Soil Micro Mechanics, Faculty of Engineering Technology, MESA+, University of Twente, Enschede, NL*
[2]*Department of Civil Engineering Indian Institute of Technology Kanpur, Kanpur, UP 208016, IN*

ABSTRACT: The study aims to develop a predictive framework for water retention in reinforced sand under partially saturated conditions. We examine how intruders like crop roots and nylon fibres modify pore size distribution and water retention in sand. Three soil configurations, bare, root-reinforced, and fibre-reinforced, were tested in laboratory-scale samples under wetting-drying cycles. Soil water retention was monitored, and soil water retention curves were fitted using the Van Genuchten model. Pore size distribution changes were quantified via X-ray computed tomography at capillary, funicular, and pendular regimes. Rooted reinforced samples were analysed, after root growth stopped, to focus only on structural effects, and compared with fibre reinforced soil of equivalent intruder length density. Rooted reinforced soil has a water storage capacity of 15-20% more than fibre reinforced or bare soils, due to larger, interconnected pores, while fibre reinforced forms isolated smaller pores. X-ray computed tomography shows pore size and connectivity changes linked to retention differences. These insights are used to validate a multiphase flow numerical model. The integrated framework will be adopted to develop a predictive model to manage drought-resilient soil.

Keywords: Sand water retention capabilities; Reinforced sand; Experimental data; X-ray computed tomography; Discrete element modelling

1 INTRODUCTION

Climate change-induced droughts pose a significant threat to global agriculture, necessitating a deeper understanding of soil-water-vegetation interactions in the vadose (unsaturated) zone (Stroosnijder et al., 2012). The study of soil water retention cuves (SWRCs) is essential for modeling water flow and solute transport in the unsaturated zone, and critical for agriculture and environmental engineering applications (Tarantino & Di Donna, 2019).

Vegetation is known to significantly alter the hydro-mechanical properties of soil (Pollen et al., 2004). Roots create a complex network of inclusions that modify the pore network architecture by forming and stabilizing macropores and increasing the tortuosity of flow paths, which directly influences water retention capabilities (Wang et al., 2025). These microstructural changes can be effectively visualized and quantified using advanced imaging techniques like X-ray computed tomography (XRCT) (Helliwell et al., 2013), and the resulting data can be used to validate numerical models of vegetated soils (e.g., Krzeminska et al., 2019).

This study presents the effects of active biological intrusions (plant roots) and inactive geometric ones (nylon fibres) on soil properties responsible for enhancing water retention. By integrating laboratory tests with imaging and numerical modeling, this research seeks to provide the path towards a comprehensive understanding of how these intrusions alter the soil's microstructure and ultimately improve its resilience to drought. This study focuses on sandy soil, a prevalent type in the western regions of the Netherlands, an area known for its agricultural importance.

2 MATERIALS AND METHODS

2.1 Experimental setup and sample preparation

We conducted laboratory tests on cylindrical sand samples (6.5 cm height, 6.6 cm diameter). The sand used was sand from the local area (Overijssel, The Netherlands), characterized by a mean particle size (D_{50}) of 0.72 mm, a coefficient of uniformity (C_u) of 2.25, a coefficient of curvature (C_c) of 0.87. The void index had a range [e_{min}, e_{max}] of 0.48, and 0.8, respectively. Samples were prepared with a consistent bulk void index of approxiamtely e=0.61 (relative density D_R=59.4%). Each sample was instrumented with both tensiometers and moisture sensors.

Three distinct soil configurations were tested namely Bare Sand (BS), Root-Reinforced Sand (RRS), Fibre-Reinforced Sand (FRS). In Figure 1 a representation of them is presented.

In RRS, *Zea mays* (corn) seeds were germinated and grown directly in the samples, which were watered with

a nutrient-enriched solution. Once the plants reached a pre-established age, the growing was stopped, and the leaves were cut to isolate the structural effects of the roots.

In FRS, Nylon fibres with diameter and length comparable to the mean root dimension of the group, were mixed into the sand prior to pluviation, to serve as passive, geometric inclusions.

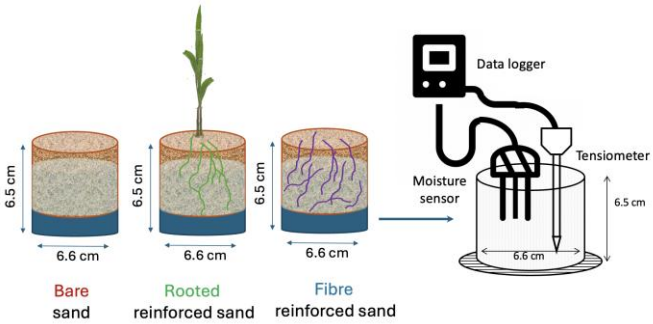

Figure 1. On the left, the representation of the bare, rooted, fibre reinforced sand samples. On the right, the representation of an instrumented sample, with the moisture sensor and tensiometer linked to a datalogger

2.2 Testing procedure

Soil water retention was monitored using the calibrated ECH20-5TM moisture sensor, and the laboratory scale Teros 31 tensiometer, both from Metergroup, to record the volumetric water content (θ), and the matric suction (ψ), see Figure 1. A series of drying-wetting cycles were performed, with the amount of cycles determined by the plant growth stage in the Root-Reinforced Sand (RRS) samples. The SWRCs were measured until the residual θ was achieved (Figure 2). After the final drying cycle, once the residual moisture content was achieved, the root systems were carefully extracted from the RRS samples to calculate the Root Length Density (RLD). This parameter is defined as the ratio between the final total length of the root system (or intrusion) components, and the volume of the soil that contains it. FRS samples were then prepared to match the Intruder Length Density (ILD) of the RRS samples, allowing for a direct comparison between roots and fibres inclusions. The geometry of the inclusion is also comparable, based on laboratory observation and literature data (Bennetzen and Hake, 2009). This analysis focuses on the drying curves, which are most relevant for understanding soil behavior during drought. Drying data were fitted using the van Genuchten model (van Genuchten, 1980). An example of the output of a RRS sample is shown in Figure 2. The reproducibility of the results was confirmed by testing multiple samples for each configuration.

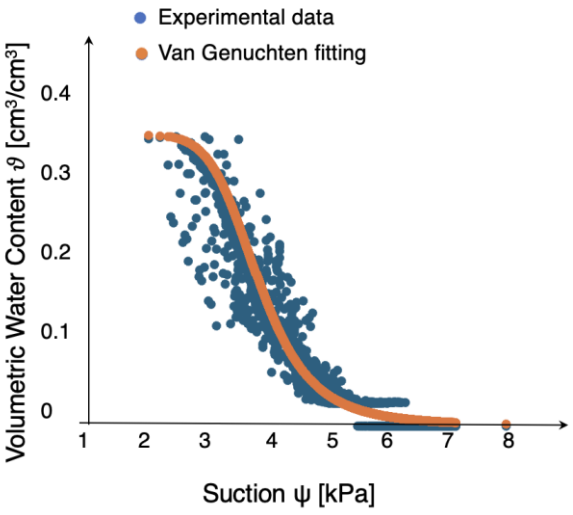

Figure 2. Experimental data and fitting curve of a RRS sample

2.3 X-ray computed tomography (XRCT)

To visualize and quantify morphologically the internal pore structure, XRCT scans were performed. The samples had all the same initial dry void index (e=0.61so we assume that changes only occur due to different inclusion quantities and water cycles. The pairs of RRS and FRS samples had equivalent intruder content. Scans were conducted at three key points on the drying SWRC: Saturation (θ_s), Transition (θ_t), and Residual (θ_r). To ensure an automatic and constituent image analysis among the scan, the reconstructed XRCT data have a pixel size of 70µm/px, hence any structural component smaller than this dimension cannot be included in the analysis. The reconstructed images were subjected to several processing steps. *3D image registration*: scans were aligned to ensure that the xyz coordinates corresponded to the same physical position within the sample in the three different scans; *Histogram normalization*: the histogram of each 32-bit scan was normalized to ensure that the same range of grey values corresponded to the same phases (i.e., sand, water, air, inclusion); *Phase segmentation*: images were segmented to assign to each pixel the corresponding unique phase.

Further details on the image processing steps are reported in Anselmucci et al., (2021).

In Figure 3, the comparison of the central vertical slices for each of the scan is reported. Each scan is taken in a specific point of the SWRC, one scan per sample for each regime. This simple, but efficient, comparison shows how the pores dry (darker grey values) as the pendular regime (θr) is approached.

3 RESULTS AND DISCUSSION

3.1 Soil water retention curves

The experimental SWRCs, fitted with the Van Genuchten model, showed that the presence of both roots and fibres enhanced water retention compared to bare sand. Plotting the effective volumetric water $\theta_{eff}= {(\theta - \theta_r)}/{(\theta_s - \theta_r)}$ content against the matric suction normalised with respect to its air entry value (ψ/ψ_{ae}) allowed for a clear comparison between samples with different initial densities and inclusion types. Figure 4a displays the comparison of SWRCs for samples with initial e=0.61, and same quantities of inclusions.

The higher is the quantity of intrusion, the higher is the retention of the soil, for both FRS and RRS. However, rooted samples (green curves in Figure 4a) showed a water storage capacity of 15-20% more than fibre-reinforced or bare soils, highlighting that the retention capability is not solely due to the geometric occlusion of pores. This suggests that the roots' influence extends beyond simple physical presence, even when the plant's hydraulic activity is stopped.

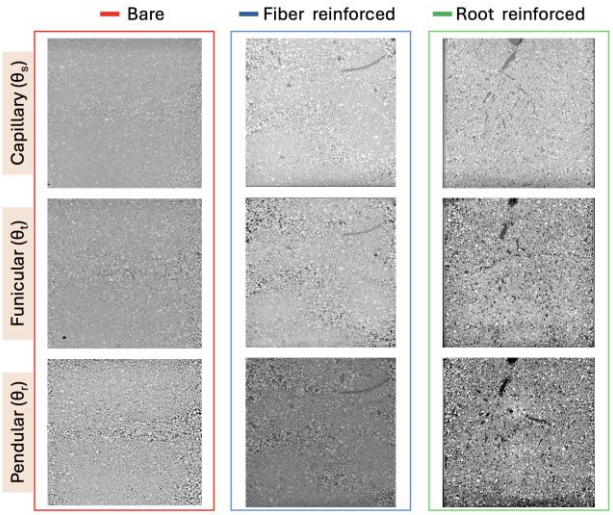

Figure 3. Comparison of vertical slices taken from the centre of the 3D cylindrical XRCT reconstruction for the bare, rooted, and fibre reinforced sample

3.2 Pore size distribution

The XRCT analysis provided direct evidence of the morphological microstructural changes induced by the inclusions. In Figure 4b, we show the pore size distribution (PSD) obtained from the XRCT scans at transition. The plot demonstrates how plant roots have higher quantity of micropores, which relates to higher value of suction needed to reach the residual water content (θ_r) compared to bare sand, and fibre-reinforced soils.

This preliminary analysis demonstrates that for the same bulk void index, the quantity of micropores produced by the inclusions (active and passive) increases up to 40% with respect to bare sand.

4 DISCRETE ELEMENT MODELLING

4.1 Pore network modelling

The experimental SWRC data are being used to calibrate a high-resolution discrete element method (DEM) model of capillary-driven drainage and imbibition (Mufti & Das, 2022). In this model, a synthetic pore network is generated and calibrated so that drainage simulations reproduce the experimentally measured soil–water retention curve (SWRC). The geometry and connectivity parameters of the pore network are optimized to achieve the best fit with experimental results and to infer pore network properties that cannot be directly measured. The model also incorporates particle size distribution from the experiments to simulate pore-scale fluid dynamics and hysteresis without relying on empirical parameters. In addition, an optimization-based pore network model (Mufti & Das, 2024) will refine the pore-throat distribution by minimizing the discrepancy between simulated and measured saturation across different suctions.

4.2 Calibration

Based on the particle size distribution and the dry bulk density of the sand samples used in the experimental campaign, the calibration of the model is obtained. Figure 5 shows the soil water retention curves, where the experimental data are compared with the output of the optimized model. The comparison is carried out for RRS and FRS samples, with same initial void index of 0.61, but different ILD. The close agreement between the two curves for both samples indicates that the optimization effectively captures the retention behaviour, with the volumetric water content decreasing as suction increases.

5 CONCLUSIONS

This study provides a preliminary view of how changes in soil microstructure, induced by either active (roots) or inactive (fibres) intruders, affects the soil water retention capabilities. The integration of experimental work SWRC data with XRCT imaging elucidated the intricate relationship between microscale modifications (pore size distribution) and macroscale hydraulic soil properties.

Our findings confirm that both roots and fibres improve the water retention of sandy soil. However, the presence of plant roots, even when their growth has stopped, enhances water retention more effectively than

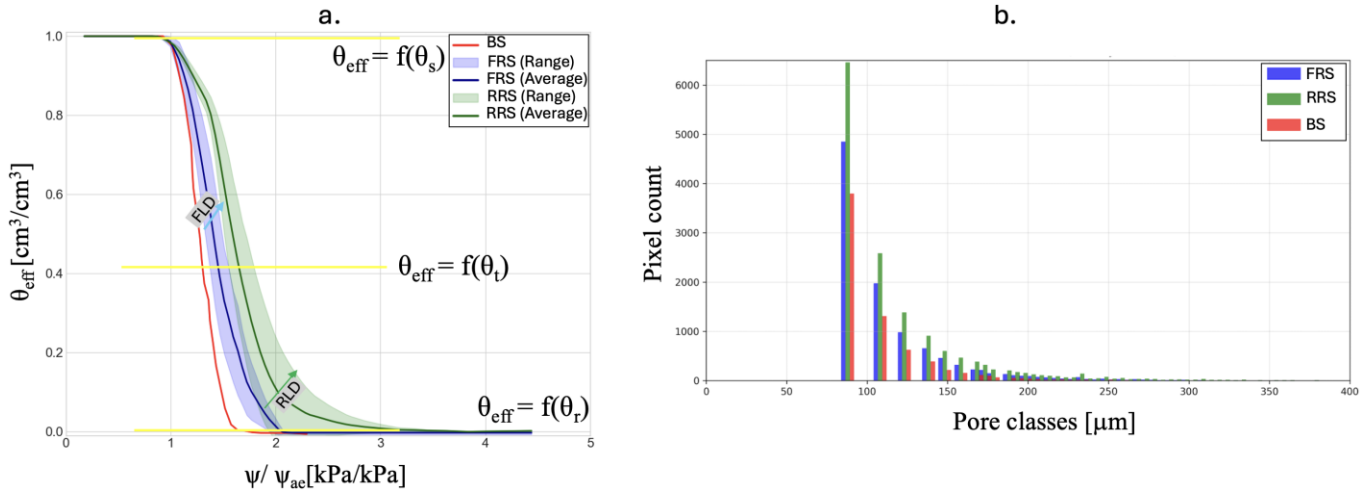

Figure 4. (a.) Comparison of the SWRCs of the bare, rooted, and fibre samples. The shadowed area represents the area occupied by the SWRCs of the specific type of sand, three samples with different quantities of inclusion inside. (b.) Pore size distribution of the three sand samples corresponding to the scans taken at the transition regime (θ_t)

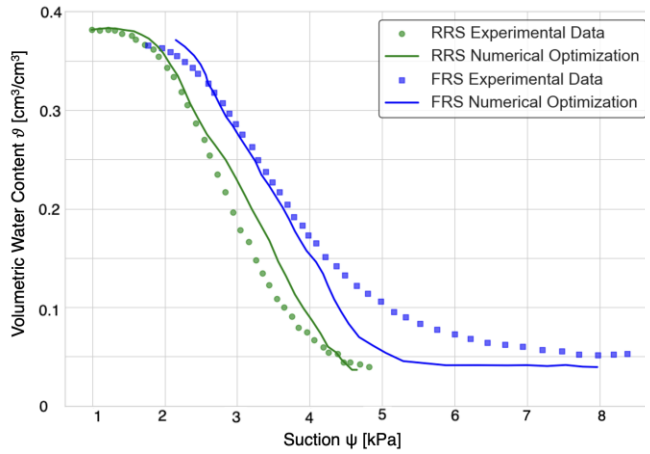

Figure 5. Comparison of the numerical optimization and the experimental data for a rooted reinforced sample and a fibred reinforced sample

synthetic fibres of an equivalent content. This is attributed to the roots' ability to create a more extensive and tortuous network of micropores, as confirmed by x-ray images, leading to higher water retention across a broader range of suction values.

The pore network model, combined with the optimisation algorithm presented will be used to obtain pore and throat radiuses and compared them with those from the x-ray images. This will help later on interpreting also more complex networks, based only on the experimental SWRCs.

6 ACKNOWLEDGEMENTS

The second and last authors would like to acknowledge the funding from the Sectorplan Beta & Techniek of the Dutch Government.

7 REFERENCES

Anselmucci, F., Andò, E., Viggiani, G., Lenoir, N., Arson, C., Sibille, L. 2021. Imaging local soil kinematics during the first days of maize root growth in sand, *Sci Rep* **11**, 22262.

Bennetzen, J.L., Hake, S.C. 2009. *Handbook of maize: its biology*. Springer, New York.

Helliwell, J.R., Sturrock, C.J., Grayling, K.M., Tracy, S.R., Flavel, R.J., Young, I.M., Whalley, W.R., Mooney, S.J. 2013. Applications of X-ray computed tomography for examining biophysical interactions and structural development in soil systems: a review, *European Journal of Soil Science* **64**(3), 279-297.

Krzeminska, D., Kerkhof, T., Skaalsveen, K., Stolte, J. 2019. Effect of riparian vegetation on stream bank stability in small agricultural catchments, *Catena* **172**, 87-96.

Mufti, S., Das, A. 2022. An advanced pore-scale model for simulating water retention characteristics in granular soils, *Journal of Hydrology* **615**, 128561.

Mufti, S., Das, A. 2024. Optimization-based pore network modeling approach for determination of hydraulic conductivity function of granular soils, *International Journal for Numerical and Analytical Methods in Geomechanics* **48**(16), 4035-4056.

Pollen, N., Simon, A., Collison, A. 2004. Advances in assessing the mechanical and hydrologic effects of riparian vegetation on streambank stability, *Riparian vegetation and fluvial geomorphology* ***8***, 125-139.

Stroosnijder, L., Moore, D., Alharbi, A., Argaman, E., Biazin, B., van den Elsen, E. 2012. Improving water use efficiency in drylands, *Current Opinion in Environmental Sustainability* **4**(5), 497-506.

Tarantino, A., Di Donna, A. 2019. Mechanics of unsaturated soils: simple approaches for routine engineering practice, *Italian Geotechnical Journal*, (4).

van Genuchten, M. T. 1980. A closed-form equation for predicting the hydraulic conductivity of unsaturated soils, *Soil Science Society of America Journal* **44**(5), 892–898.

Wang, X., Liu, S., Lan, H., Sun, W., Ren, X., Li, Z. 2025. Research of unsaturated strength characteristics for root–soil composite under different water content conditions, *Scientific Reports* **15**(1), 22516.